JOURNAL OF MATERIALS SCIENCE **35** (2000) 5415–5420

Preparation of nanosized $LaCoO_3$ perovskite oxide using amorphous heteronuclear complex as a precursor at low temperature

YONGFA ZHU*, RUIQIN TAN
Department of Chemistry, Tsinghua University, Beijing 100084, People's Republic of China
E-mail: zhuyf@chem.tsinghua.edu.cn

TAO YI
State Key Laboratory of Rare Earth Materials Chemistry and Application, Peking University, Beijing 100871, People's Republic of China

SHISHAN JI, XIAOYAN YE, LILI CAO
Department of Chemistry, Tsinghua University, Beijing 100084, People's Republic of China

---

Nanosized $LaCoO_3$ cobaltite oxide powder with perovskite structure was successfully synthesized at a relatively low calcination temperature using an amorphous heteronuclear complex, $LaCo(DTPA)\cdot 6H_2O$, as a precursor. The precursor decomposed completely into cobaltite oxide above 400 °C according to the DTA and TGA results. XPS revealed that the decomposed species was composed of $LaCoO_3$ cobaltite oxide after the precursor was calcined at 500 °C for 2 hours. XRD demonstrated that nanosized $LaCoO_3$ crystalline powder with perovskite structure was formed after the calcination temperature increased to 600 °C. The grain size and the crystal size of $LaCoO_3$ increased with the calcination temperature from 500 °C to 800 °C, and the heat-treatment time has a less obvious effect on the grain size and the crystal size. It is a useful way to synthesize nanosized perovskite oxides using an amorphous complex as a precursor. This method can be easily quantitatively controlled.

---

1. Introduction

Perovskite oxides have caused great interests and have been widely studied for their various properties and application in the recent decades. They can be used as superconductors, and the critical temperature decreases linearly with increasing A-site disorder, as quantified by the variance in the distribution of A-site cation radii. The critical temperature is also very sensitive to lattice strains [1]. $(RE)CoO_3$ perovskites have a variety of the magnetic and electrical characteristics. They show a semiconductor behavior below the room temperature [2, 3]. The catalytic properties of perovskite oxides also make them effective in various oxidation and reduction reactions [4]. They have been considered as a promising substitute of the classical Pt/Rh-based catalysts applied in the automotive pollution control [5–7]. In addition, perovskite oxides are also a good electrode material for secondary batteries and fuel batteries [8, 9].

Different preparation methods of the perovskite oxides result in different physical or even chemical properties of these materials. These methods include co-melting, freeze-drying, spray-drying, precipitation, Sol-Gel, *et al.* [10, 11]. It has been reported that the catalytic activity of some materials prepared by different methods has the following sequence: freeze-drying>spray-drying>precipition [12]. Nanosized particles and thin films are not easily obtained by the traditional methods. It has been shown that the co-melting method by solid state reaction need a temperature as high as about 1050 °C. It is difficult to synthesize nanosized materials by this method. Sol-Gel method has been widely used to prepare nanosized materials, but its application is limited by the stability of its precursor system and it is difficult to control the chemical composition of complicated oxides [13].

In this paper, a new preparation method was established using an amorphous heteronuclear complex as a precursor to prepare the nanosized perovskite oxide $LaCoO_3$. The crystalline phase with perovskite structure was obtained after the precursor was calcined at 600 °C for 1 hour. The particle size and crystal size increased with the calcination temperature and time. It is proved that the heteronuclear complex can decompose and form oxides at relatively low temperature compared with the traditional methods. It is much easier to prepare complicated oxides using complex precursors because they can be synthesized more easily and the chemical composition can be controlled more quantitatively.

---

[*] Author to whom correspondence should be addressed.

0022–2461

2. Experimental

2.1. The synthesis of LaCo(DTPA)·6H_2O precursor

Firstly, NaOH solution with 1.0 mol/l concentration was added in drops into the mixture solution of $La(NO_3)_3$ and $CoCl_2$ to prepare the fresh $La(OH)_3$ and $Co(OH)_2$ depositions. Then, Diethylenetriamine-pentaacetic acid (H_5DTPA) with calculated molar ratio was mixed with these fresh $La(OH)_3$ and $Co(OH)_2$ in water to synthesize the complex precursor. The mixture was stirred and heated to 80 °C to promote the reaction of the mixture. After the mixture became a transparent solution, it was vaporized slowly at room temperature until a piece of transparent glasslike material was formed. The precursor was obtained after the solution was dried completely. The result of element analysis showed that the possible formula of the precursor was LaCo(DTPA)·6H_2O. XRD pattern demonstrated that the complex precursor was amorphous.

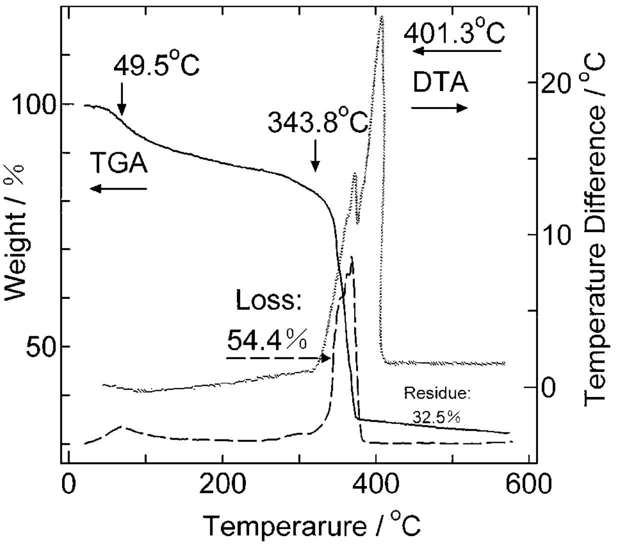

Figure 1 The TGA and DTA spectra of LaCo(DTPA)·6H_2O precursor.

2.2. The preparation of $LaCoO_3$ cobaltite compound

The $LaCoO_3$ cobaltite oxide was prepared by decomposing the precursor in air. At first, the temperature was raised to 300 °C at a slow heating rate (6 °C/min). The temperature was maintained for 90 minutes to promote the decomposition of organic components. Then, the temperature increased to various pre-set temperature and maintained for a definite period of time to promote the formation of cobaltite oxide.

2.3. Experimental techniques

XRD experiments were carried out in Rigaku DMAX-2400 diffractometer with Cu K_α radiation. The grain size was measured using Hitachi H-800 Transmission Electron Microscopy (TEM). The accelerating voltage of electron beam was 200 kV. TGA and DTA analysis were performed on a Dupond 1090 thermal analyzer. The atmosphere was air, and the heating rate was 10 °C/min. The XPS spectra were measured in a PHI 5300 ESCA system. A Al K_α X-ray source with a power of 250 W was used. The pass energy of the analyzer was set at 37.25 eV and the base pressure of the analysis chamber was better than 4×10^{-8} torr. The charge effect was calibrated using the binding energy of C 1s [14].

3. Results and discussion

3.1. The thermal decomposition

The results of TGA and DTA for LaCo(DTPA)·6H_2O complex are shown in Fig. 1. The change of residual weight with temperature was shown by the solid curve and the thermal change with temperature was shown by the dot curve. The dash curve showed the differential of the weight loss. With the temperature rising, three weight loss regions were observed in the solid curve. According to the quantitative calculation of the weight loss in each region, the thermal decomposition processes were distinguished as followings. The weight loss region from 20 °C to 90 °C resulted from the loss of coordinated water. The region of weight loss from 90 °C to 340 °C was attributed to the decomposition of hydrocarbon and amino-group organic components. The strong weight loss region from 343.8 °C to 370 °C was attributed to the decomposition of carboxyl cobalt group and carboxyl lanthanum group. No further peak or weight loss appears thereafter, indicating that all organic components have been eliminated. The decomposition temperature of carboxyl cobalt group and carboxyl lanthanum group was very close, which may be helpful for the formation of cobaltite oxide. Two exothermic peaks were observed on the DTA curve. The peak at 366.5 °C was attributed to the decomposition of carboxyl cobalt and carboxyl lanthanum group. The peak at 401.3 °C was very strong, and no weight loss was corresponded to it, implying that this peak resulted from the formation of $LaCoO_3$ cobaltite oxide. The results above suggest that $LaCoO_3$ oxide can be formed below 500 °C by decomposing an amorphous complex of LaCo(DTPA)·6H_2O.

3.2. The crystallization of $LaCoO_3$ compound

The influence of the calcination temperature on the formation of $LaCoO_3$ crystalline phase has been investigated using XRD. The XRD patterns of $LaCoO_3$ samples calcined at different temperature are shown in Fig. 2. After the precursor was calcined at 500 °C for 2 hours, the XRD pattern showed that the sample was still amorphous. Several sharp peaks were observed after the precursor was calcined at 600 °C for 2 hours. According to the XRD standard spectra of $LaCoO_3$ crystal, these peaks were attributed to the pure perovskite-type $LaCoO_3$ crystal. This result indicated that $LaCoO_3$ with pure perovskite structure can be synthesized by this way at 600 °C. With the calcination temperature rising, the peak intensified significantly and some peaks even split in half. The peaks of perovskite also became sharper with the annealing temperature. This can be explained that the crystalline phase of $LaCoO_3$ became more perfect with the calcination temperature.

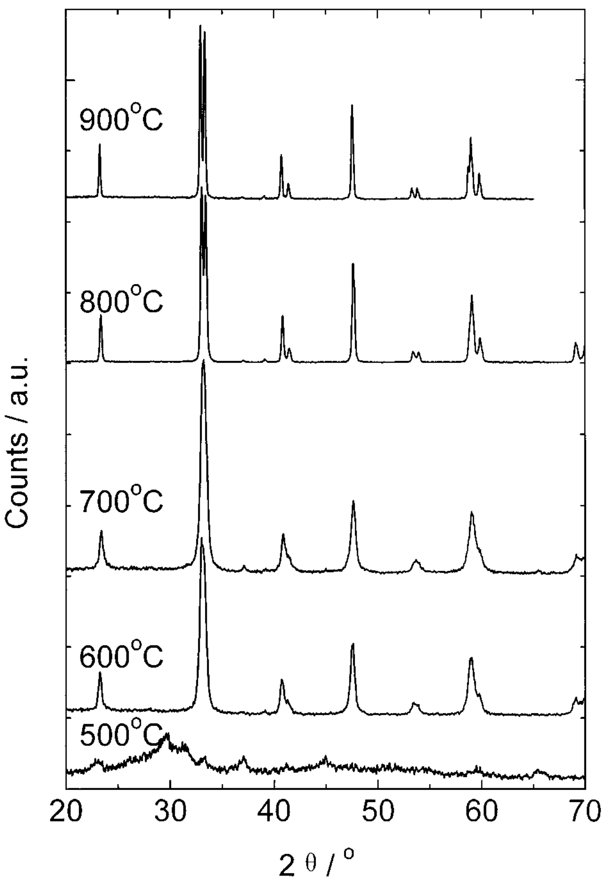

Figure 2 The XRD patterns of samples calcined at different temperature for 2 hours.

The influence of calcination time on the formation of $LaCoO_3$ crystalline phase was also studied by XRD. As it was shown in Fig. 3, the perovskite crystalline phase has formed after the precursor was calcined at 600 °C for 1 hour, accompanied with some tiny peaks due to some amorphous intermediate ($2\theta = 29°$). They disappeared with the increasing of the calcination time. The peaks of the crystalline phase only became a little sharper and did not change much with the calcination time.

The results above indicated that $LaCoO_3$ crystalline phase can be formed at a relative low temperature (600 °C) using an amorphous complex as a precursor. The influence of the calcination temperature is much more significant than that of the calcination time.

3.3. The identification of $LaCoO_3$ species

The chemical compositions of decomposed samples have been determined using XPS. The spectra of Co 2p in the decomposed samples calcined at 500 °C and 600 °C for two hours are shown in Fig. 4. The binding energies of Co $2p_{3/2}$ in Co_2O_3, Co_3O_4 and CoO oxides were 779.6, 779.8 and 780.4 eV, respectively [14]. The binding energies of Co $2p_{3/2}$ in the samples decomposed at 500 °C and 600 °C were 779.1 and 778.8 eV respectively, which was lower than that in cobalt oxides. This result indicated that Co atoms did not exist as simple cobalt oxides in decomposed samples. Furthermore, the line shapes of Co 2p in the decomposed samples calcined at 500 °C and 600 °C were different from that in Co_3O_4. The Co 2p line of these species also exhibited a satellite band as CoO oxide. It has been shown that high spin cobalt(II) compounds have intense satellite bands associated with Co 3s and Co $2p_{3/2}$ lines, while the satellite lines for the low spin cobalt(III) compounds are either weak or missing [15]. It also has been shown that the Co 2p spin-orbit splitting is affected by the net

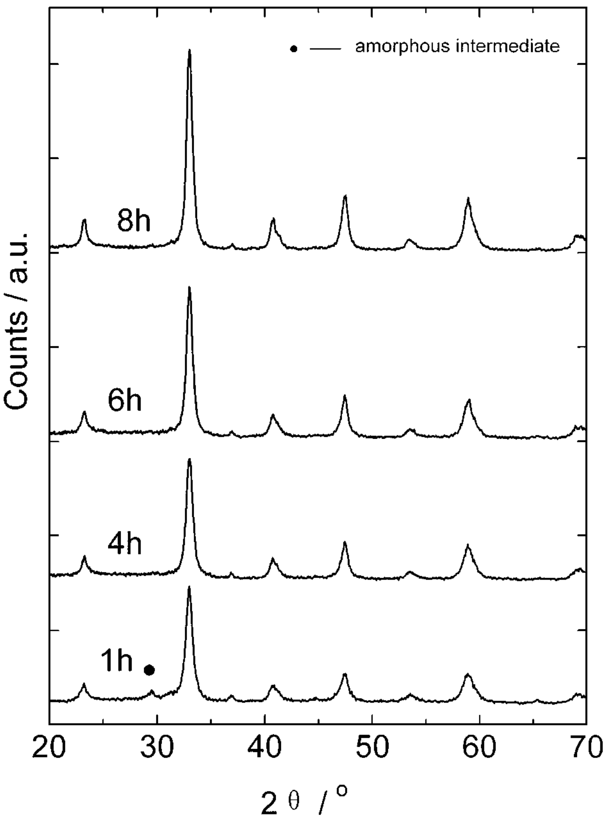

Figure 3 The XRD patterns of samples calcined at 600 °C for various time.

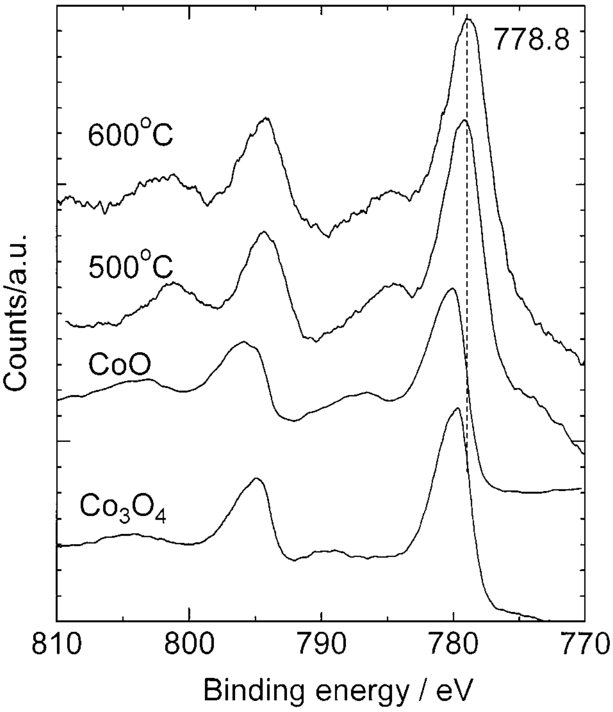

Figure 4 The Co 2p spectra of the sample calcined at 500 °C and 600°C for 2 hours.

spin of the cobalt complex. This probably results from multiplet splitting of the Co 2p lines for the high spin compounds which in turn, may be responsible for the broader Co 2p line widths for this compound. Based on the results of Co 2p, it can be considered that Co existed as the cobaltite compound in decomposed samples. It can be concluded from the above results that the precursor can be decomposed into $LaCoO_3$ compound even if calcined at 600 °C in air.

The O 1s spectrum consists of two distinct oxygen peaks. The binding energies are 528.7 eV corresponding to La-O band and 531.4 eV corresponding to Co-O band respectively. This result shows that there are two chemical environments of O element in this perovskite oxide. The lower value is similar with that of La_2O_3 (528.6 eV) and the other is higher than those in the simple oxides of CoO (530.1 eV), Co_2O_3 (529.6 eV), Co_3O_4 (530.2 eV) [14]. This implys that O 2p orbit obtains less electron charges from Co valence orbit in $LaCoO_3$ than in monoxides.

The binding energies of La 3d in pure La and La_2O_3 compounds were 835.8 eV and 833.7 eV respectively [14]. The binding energy of La 3d in decomposed sample annealed at 600 °C for 2 hours was 833.1 eV. It showed that La element in the perovskite oxide had stronger polarization ability and a more remarkable relaxation phenomenon. This result suggested that the decomposed sample was cobaltite oxide. It can be concluded from the above results that the precursor can be decomposed into $LaCoO_3$ oxide after it is calcinated at a temperature above 600 °C in air.

3.4. The grain size and crystal size of $LaCoO_3$ species

The grain size of $LaCoO_3$ compound varied with calcination temperature has been studied using TEM as shown in Fig. 5. The grain edge of the sample calcined at 500 °C for 2 hours was a little dim as Fig. 5a showed. It indicated that the sample was still amorphous at this temperature. This result agreed with that obtained by XRD. The photos also showed that the grain size was homogenous and fairly small when the sample was obtained at a lower calcination temperature such as 600 °C (Fig. 5b) and 700 °C. The grain sizes grew quickly after the precursors were calcined at a much higher temperature. It showed in Fig. 5c that the grain size was much bigger after the sample was calcined at 800 °C for 2 hours. The dependence of the average grain size on the heat-treatment time was also investigated at 600 °C. The TEM photos show that the heat-treatment time has a less obvious effect on the grain size of the powder. The samples calcined for 1 hour (Fig. 5d), 2 hours and 4 hours (Fig. 5e) separately have the similar grain size. Even when the sample was calcined for 6 hours, the grain size didn't change too much. But it began to gather. After it was calcined for 8 hours, it resulted in the formation of coarse aggregation (Fig. 5f).

The activation energies of the grain size and crystal size growth can be calculated according to the Burke equation: $D^2 - D_0^2 = K_0 t^n \exp(-Q/RT)$ [16]. D is the grain or crystal size after calcined; D_0 is the original size; K_0 is a constant. t is the calcination time; 2 hours; n is the time index, 1. It can be deduced that: $\ln D = A - Q/(2RT)$, $A = \ln 4K_0/2$. There exists a linear relationship between $\ln D$ and $1/T$. The slope is $(-Q/2R)$. It was obtained that the activation energy of the grain size growth was $96.75\text{k} \cdot \text{mol}^{-1}$ and the activation energy of the crystal size growth was $42.44\,\text{kJ} \cdot \text{mol}^{-1}$.

TABLE I The dependence of grain sizes and crystal sizes on the calcination temperature which were determined from TEM photos and derived from XRD patterns

Temperature/°C, for 2 hours	500 °C	600 °C	700 °C	800 °C	900 °C
Average grain size, Dg/nm	15–20	20	25	100–150	200
Average crystal size, Dc/nm	Amorphous	15.3	18.6	23.7	32.8

TABLE II The dependence of grain sizes on the heat-treatment time determined from TEM photos and the crystal sizes derived from XRD patterns

Heat-treatment time/h, 600°C	1	4	6	8
Average grain size, Dg/nm	10–15	15–20	20–25	25–30
Average crystal size, Dc/nm	9.65	13.0	13.7	13.7

TABLE III The specific surface areas measured by BET

Sample	500 °C, 2 h	800 °C, 2 h	600 °C, 1 h	600 °C, 4 h	600 °C, 6 h
Specific surface area/$m^2 \cdot g^{-1}$	19.34	3.77	17.86	15.41	14.90

The average crystal sizes can be determined from the XRD pattern parameters according to the Scherrer equation: $\text{Dc} = K\lambda/\beta \cos\theta$. Dc is the average crystal size, K is the Scherrer constant equal to 0.89, λ is the X-ray wavelength equal to 0.1542 nm, and β is the full width at half-maximum (FWHM) and θ is the diffraction angle [11]. The results are both shown in Tables I and II. It reveals that the calcination temperature has a significant influence on the average crystal size, while the crystal size does not change too much with the calcination time at 600 °C.

The specific surface areas of some samples were measured by BET method. The results are listed in Table III. The sample calcined at 500 °C for 2 hours had a larger specific surface area because the sample existed as amorphous and the grain size was smaller. With the rising of the calcination temperature, the specific surface area decreased significantly. These results also indicated that the specific surface area became smaller with the rising of the calcination time, as well as with the rising of the calcination temperature. The change of the specific surface area was relative with that of grain size and the crystal size. It obviously showed that the larger the grain size and crystal size the smaller the specific surface area.

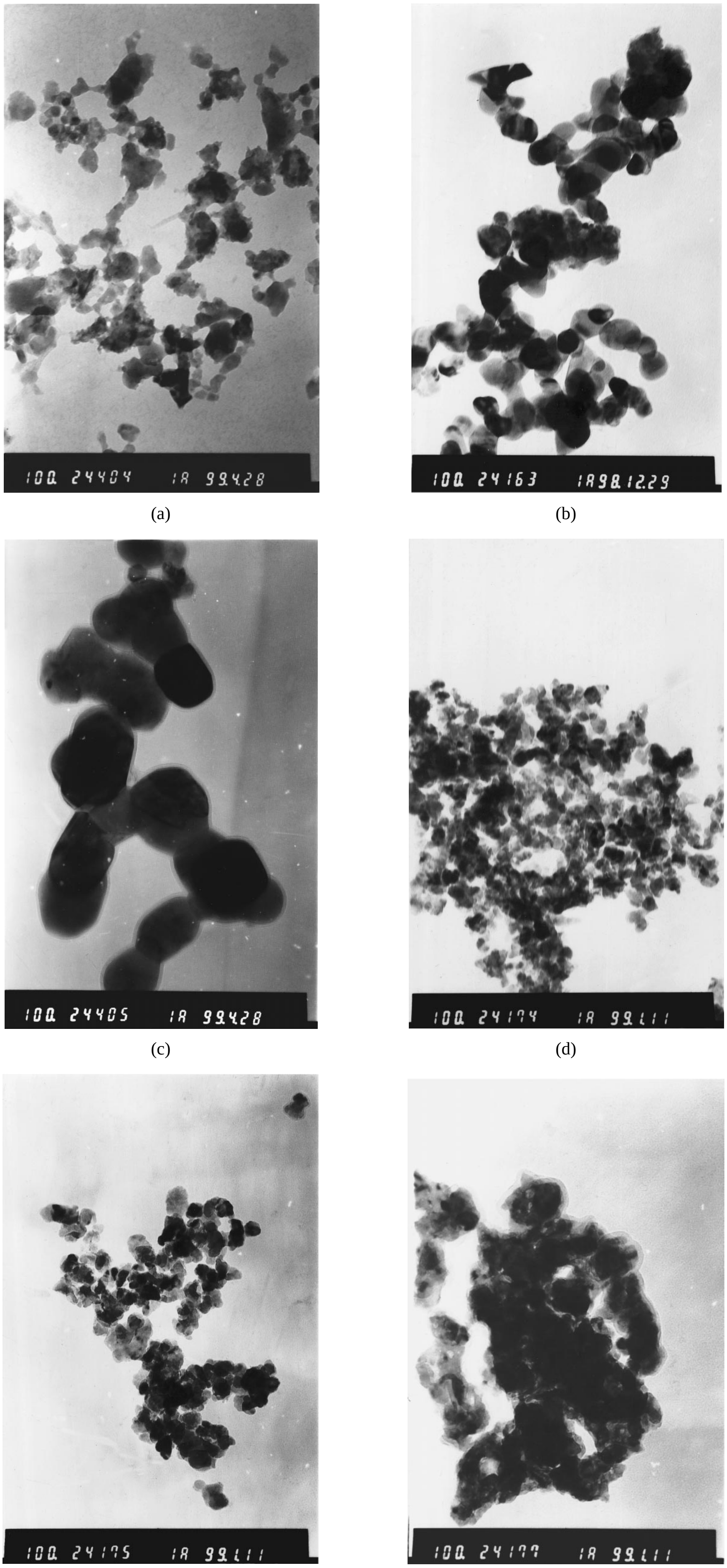

(a) (b)

(c) (d)

(e) (f)

Figure 5 The TEM photos of the calcined samples. (a) The sample calcined at 500 °C for 2 hours (100,000 times); (b) The sample calcined at 600 °C for 2 hours (100,000 times); (c) The sample calcined at 800 °C for 2 hours (100,000 times); (d) The sample calcined at 600 °C for 1 hour (100,000 times); (e) The sample calcined at 600 °C for 4 hours (100,000 times); (f) The sample calcined at 600 °C for 8 hours (100,000 times).

4. Conclusions

(1) Nanosized $LaCoO_3$ cobaltite oxide was synthesized using amorphous heteronuclear complex $LaCo(DTPA)\cdot 6H_2O$ as a precursor at a relative low calcination temperature. To form perovskite crystalline phase of $LaCoO_3$, the calcination temperature should be higher than 600 °C. This work proved it was an effective method to synthesized nanosized $LaCoO_3$ oxide using amorphous heteronuclear complex as a precursor.

(2) The grain size is in nano-scale if the precursor is calcined at relatively low calcination temperature. The grain size grows dramatically with the calcination temperature above 800 °C and also increases with the calcination time.

References

1. J. P. ATTFIELD, A. L. KHARLANOV and J. A. McALLISTER, *Nature* **394** (1998) 157.
2. K. ASAI *et al*., *Phys. Rev. B* **50** (1994) 3025.
3. S. YAMAGUCHI, Y. OKIMOTO and Y. TOKURA, *ibid*. **54** (1996) 11022.
4. L. G. TEJUCA, J. L. G. FIERRO and J. M. D. TASCON, "Advanced Catalysis" (Academic Press, San Diego, 1998) p. 237.
5. D. B. MEADOWCROFT, *Nature* **226** (1970) 847.
6. N. MIZUNO and M. YAMATO *et al*., *J. Catal*. **132** (1991) 560.
7. J. A. ANDERSON and J. L. G. FIERRO, *J. Solid State Chem*. **108** (1994) 305.
8. S. B. ADLER, J. A. LANE and B. C. H. STEELE, *J. Electrochem. Soc*. **143**(11) (1996) 3554.
9. D. W. JOHNSON, JR., P. K. GALLAGHER, F. SCHREY and W. W. RHODES, *Am. Ceram. Soc. Bull*. **55** (1976) 520.
10. L. SIMONOT, F. GARIN and G. MAIRE, *Applied Catalysis B: Environmental* **11** (1997) 181.
11. G. XIONG, ZHENG-LIANG ZHI and XUJIE YANG *et al*., *J. Mater. Scien. Lett*. **16** (1997) 1064.
12. N. MIZUNO *et al*., *Catalysis Today* **8** (1990) 221.
13. M. GUGLIELMI and G. CARTURAN, *Joural of Non-Crystalline Solids* **100** (1988) 16.
14. J. F. MOULDER, W. F. STICKLE, P. E. SOBOL and K. D. BOMBEN, in "Handbook of X-ray Photoelectron Spectroscopy," edited by J. Chastain (Perkin-Elmer Corporation, Eden Prairie, MN, 1992).
15. N. S. MCLNTYRE and M. G. COOK, *Analytical Chemistry* **47**(13) (1975) 2208.
16. QIAN YITAI, "Crystallization Chemistry" (The Science and Technology University of China Publishing House, Beijing, 1988) p. 140.

Received 7 July 1999
and accepted 28 March 2000